A theoretical and experimental NMR study of the tautomerism of two phenylene-bis-*C*-substituted pyrazoles†

Dionisia Sanz,*[a] Rosa M. Claramunt,[a] Ibon Alkorta,[b] José Elguero,[b] Werner R. Thiel[c] and Tobias Rüffer[d]

Received (in Montpellier, France) 5th March 2008, Accepted 18th June 2008
First published as an Advance Article on the web 3rd September 2008
DOI: 10.1039/b803855d

Two bis-pyrazolylbenzenes, one *meta*- and the other *para*-substituted, have been studied by multinuclear magnetic resonance both in solution and in the solid state, including ^{13}C CP-MAS NMR variable temperature experiments. The tautomerism in DMSO-d_6 solution has been studied and the most stable tautomers (the 3,3 and the 3,5) identified. In the solid state the *meta* derivative exists as the 3,3-tautomer while the tautomer of the *para* derivative is the 3,5 one. This latter tautomer exists in a dynamic equilibrium with the 5,3 one, representing a new and original example of proton transfer in the solid state (SSPT).

Introduction

The annular tautomerism of *N*-unsubstituted pyrazoles is a classical problem in heterocyclic chemistry.[1] We have contributed to this subject for a long time; for some recent papers by our and other groups, see respectively, refs. 2 and 3.

Besides the thermodynamic aspect, *i.e.* the determination of equilibrium constants, there is the kinetic part of the problem concerning the rates of proton transfer. Both aspects are especially interesting in the solid state, the first one being better approached by X-ray crystallography and the second one, when it occurs, by solid-state NMR spectroscopy (solid-state proton transfer, SSPT).

For SSPT to occur in *NH*-pyrazoles, two conditions are necessary but not sufficient: (i) that they crystallize forming cyclic structures (cyclamers)[4] and (ii) that the substituents at positions 3 and 5 of the pyrazole ring are identical or, at least, similar.[5] As shown in Scheme 1, after a double, triple or quadruple proton transfer an identical, albeit rotated, structure is obtained.

However, if this is the only possibility for dimers and trimers, in the case of tetramers, it is possible to obtain the *same* structure after a quadruple proton transfer, *even* if the substituents at positions **3** and **5** are different (Scheme 2).[6]

There is a second unexplored possibility to obtain an identical structure after SSPT: to have an *even* number, for instance two, of *NH*-pyrazole rings as 3(5)-substituents in the *same* molecule. If these compounds form cyclamers involving both pyrazole rings, one as 3-substituted and the other as a 5-substituted *NH*-pyrazole then, after proton transfer, the same structure will be obtained (see Scheme 3 for a dimer).

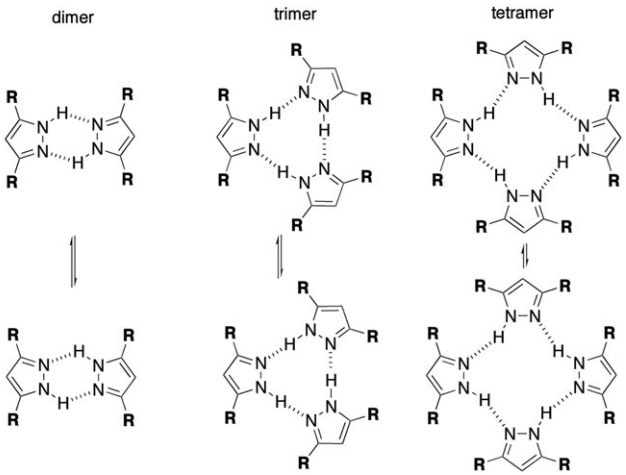

Scheme 1 Proton transfer in pyrazole cyclamers.

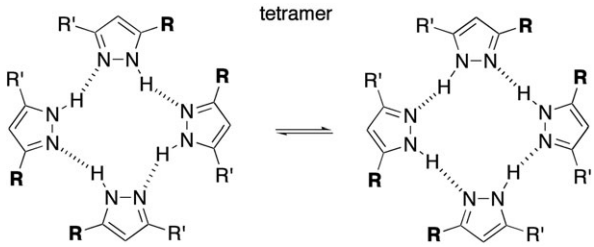

Scheme 2 Quadruple proton transfer in asymmetric pyrazole tetramers.

We decided to study the case of molecules having two *NH*-pyrazoles linked through a phenyl ring, either in *meta* **1** or in *para* positions **2** (Scheme 4). These molecules present four tautomers, two being degenerate: **a** (3,3), **b** (3,5), **b′** (5,3) and **c** (5,5). Only tautomers **b** and **b′** satisfy the condition for SSPT. Since **b** and **b′** are identical, we will use **b** for both of them.

[a] *Departamento de Química Orgánica y Bio-Orgánica, Facultad de Ciencias, UNED, Senda del Rey 9, E-28040 Madrid, Spain. E-mail: dsanz@ccia.uned.es*
[b] *Instituto de Química Médica, CSIC, Juan de la Cierva 3, E-28006 Madrid, Spain. E-mail: ibon@iqm.csic.es*
[c] *Fachbereich Chemie, Technische Universität Kaiserslautern, Erwin-Schrödinger-Str. Geb. 54, D-67663 Kaiserslautern, Germany. E-mail: thiel@chemie.uni-kl.de*
[d] *Institut für Chemie, Technische Universität Chemnitz, D-09107 Chemnitz, Germany. E-mail: Tobias.rueffer@chemie.tu-chemnitz.de*

† Electronic supplementary information (ESI) available: Details on theoretical calculations. CCDC reference numbers 679321 (**1**) and 679322 (**2**). For ESI and crystallographic data in CIF or other electronic format see DOI: 10.1039/b803855d

Scheme 3 Hypothetical example of double SSPT leading to an identical structure.

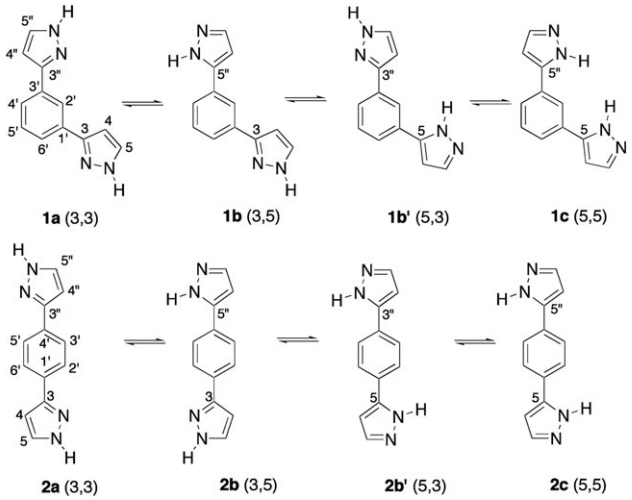

Scheme 4 The tautomerism of 3,3′-(1,3-phenylene)bis-1*H*-pyrazole (**1a**) and 3,3′-(1,4-phenylene)bis-1*H*-pyrazole (**2a**).

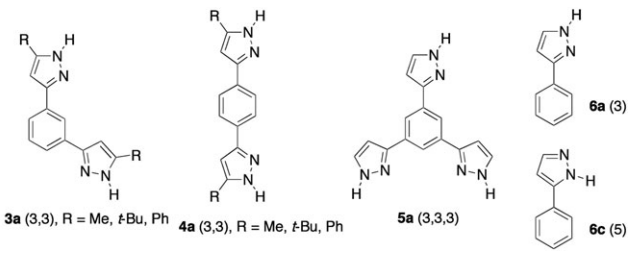

Scheme 5 Other bis- and tris-pyrazolylbenzenes.

Results and discussion

Phenylenebispyrazoles **1** (CAS registry number 293750-75-1) and **2** (CAS registry number 63285-56-3) are relatively unexplored compounds. Compound **2** was prepared by Lin and Lang in 1977[7] while compound **1** was first described in a 2000 patent[8] and the following year Thiel and co-workers reported the synthesis of both **1** and **2**.[9] More recently, similar compounds **3** and **4** but with the pyrazoles bearing substituents were synthesized by Hayter, Bray, Clegg and Lindoy (Scheme 5).[10] Finally, Thiel and co-workers also prepared the tris-derivative **5**.[9,11] The tautomerism of none of these compounds were examined.

Theoretical calculations

We have calculated the energies (including the ZPE correction) and absolute shieldings (σ, ppm) of compounds **1a**, **1b** (**1b′**), **1c**, **2a**, **2b** (**2b′**) and **2c** both in the gas phase and solvated by DMSO (PCM model). In order to determine if both pyrazole rings in **1** and **2** are independent or if their tautomerism is related, we have calculated at the same level the case of 3(5)-phenylpyrazole (**6**) [**6a**, 3-phenyl and **6c** 5-phenyl tautomer].[12] The geometry of the complexes has been optimized at the B3LYP/6-31G(d) and B3LYP/6-311++G(d,p) computational levels. The absolute chemical shieldings have been obtained at the B3LYP/6-311++G(d,p) level using the GIAO method (see Experimental section).

The energies are reported in Table 1. The minimum energy conformations are as represented in Scheme 4: **1a** *Z*,*E*, **1b** *E*,*E*, **1c** *Z*,*Z*; **2a** *E*,*E*, **2b** *Z*,*Z*, **2c** *E*,*E*. We have used the *E*/*Z* descriptors to define the conformations about the pyrazole–phenyl bond (atropisomers) of compounds **1** and **2**.

In the gas phase, the lack of additivity is evident: the **c** tautomers (5,5-diaryl) are less favorable than twice 1.42 kJ mol^{-1} (5-monoaryl) and the mixed tautomers **b** are not the average of **a** and **c** (**1**: 2.64 instead of 1.12; **2**: 2.27 instead of 0.59). The inclusion of solvent effects (PCM model with DMSO) increases the differences of energy with regard to **a** tautomers, the **b** tautomers are in the average of **a** and **c** (**1**: 4.57 instead of 4.68; **2**: 4.34 instead of 3.69). In both conditions, it appears that tautomers **c**, higher in energy, can be excluded from the tautomeric mixtures. We have calculated the percentages at 298.15 °C corresponding to these calculations. For the *meta* compound in the gas-phase (1.12 kJ mol^{-1}): 44.0% (**1a**), 56.0% (**1b** + **1b′**); for the *para* compound in the gas phase (0.59 kJ mol^{-1}): 38.8% (**2a**), 61.2% (**2b** + **2b′**); for the *meta* compound in DMSO (4.68 kJ mol^{-1}): 76.8% (**1a**), 23.2% (**1b** + **1b′**), and for the *para* compound in the DMSO (3.69 kJ mol^{-1}): 68.9% (**2a**), 31.1% (**2b** + **2b′**).

We have transformed the calculated σ values into chemical shifts (δ/ppm) using three empirical relationships we have

Table 1 Absolute (hartrees) and relative energies (kJ mol^{-1}) of the different arylpyrazole tautomers including ZPE corrections

Pyrazole	E_{total}	E_{rel}	Pyrazole	E_{total}	E_{rel}	Pyrazole	E_{total}	E_{rel}
Gas phase								
6a	−457.38109	0.00	**1a**	−682.45098	0.00	**2a**	−682.45133	0.00
6c	−457.38055	1.42	**1b**	−682.45056	1.12	**2b**	−682.45110	0.59
			1c	−682.44897	5.28	**2c**	−682.44960	4.54
DMSO								
6a	−457.39375	0.00	**1a**	−682.47339	0.00	**2a**	−682.47443	0.00
6c	−457.39231	3.75	**1b**	−682.47160	4.68	**2b**	−682.47302	3.69
			1c	−682.46991	9.14	**2c**	−682.47113	8.67

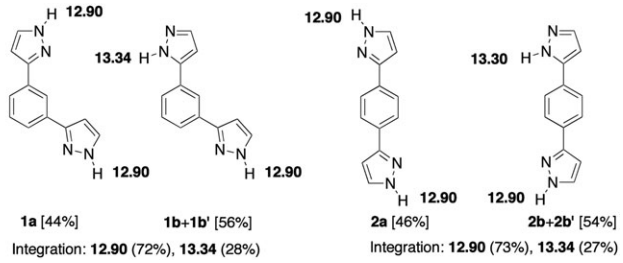

Scheme 6 ^{1}H NMR signals of the *NH* groups.

devised for a large series of compounds:[13,14] $\delta(^{1}H) = 30.6 - 0.953\sigma(^{1}H)$ $\delta(^{13}C) = 175.7 - 0.962\sigma(^{13}C)$ $\delta(^{15}N) = -152.0 - 0.946\sigma(^{15}N)$, and used these calculated δ values to perform an independent assignment of the different signals, which is based on 2D experiments. Both assignments coincide.

Experimental NMR study in solution

(a) ^{1}H NMR. The ^{1}H NMR spectra in DMSO-d_6 (15.5 mg in 0.5 mL of solvent) of compounds **1** and **2** show the presence of tautomers **a** and **b** in an almost 1 : 1 ratio (actually 44 : 56 and 46 : 54 for **1** and **2**, respectively, see Scheme 6).

The gas-phase calculations (44 : 56 and 39 : 61) reproduce very well the experimental results (44 : 56 and 46 : 54), not so the PCM ones (77 : 23 and 69 : 31) that exaggerate the stability of the **a** tautomers.

(b) ^{13}C NMR. In ^{13}C NMR in DMSO-d_6 at identical concentration than in ^{1}H NMR the **a** : **b** proportions ought to be the same. The problem is that there are few different signals to identify the tautomers and besides one pyrazole ring is almost independent of the other, so many signals are identical for the 3-aryl moiety. However, thanks to the combined use of 2D experiments and theoretical calculations all signals have been unambiguously identified. Some of them are broad indicating a tautomerization process.

(c) ^{15}N NMR. Although the signals corresponding to N2 are not observed (being probably too broad) those of N1 are very similar for both compounds and both tautomers (Scheme 7).

Experimental NMR study in the solid state

(a) ^{13}C NMR. In the solid state, the ^{13}C NMR spectrum of compound **1** (without NQS) is represented in Fig. 1. This compound always crystallizes with solvent molecules (ethyl acetate, diethyl ether, chloroform, ...) that cannot be eliminated under vacuum and medium heating (50 °C). The ^{13}C NMR signals of the compound are always identical whatever

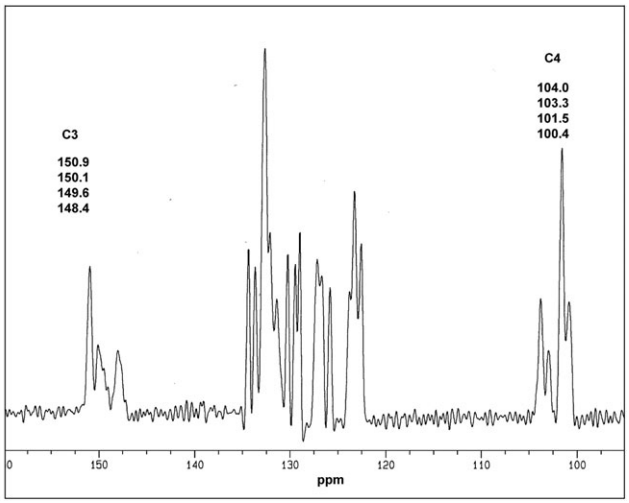

Fig. 1 ^{13}C CP-MAS spectra of **1**.

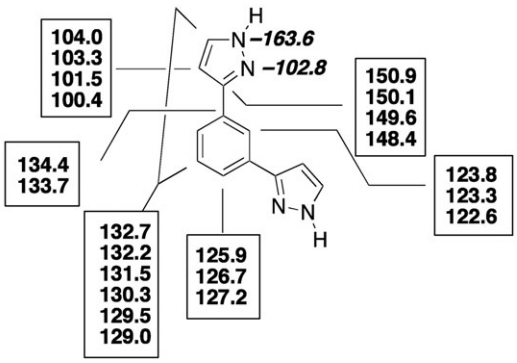

Scheme 8 ^{13}C and ^{15}N CP-MAS chemical shifts of tautomer **1a**.

the guest. They show an important splitting but all of them belong to tautomer **1a**, for instance, the signals at 139.8 and 142.0 typical of **1b** (Scheme 7) are absent. Therefore, compound **1** in the solid state should exist in the form of **1a** but with several independent molecules (possibly six considering that all the signals should have the same intensity) (Scheme 8).

The behavior of compound **2** is very different. The signals of the ^{13}C CP-MAS NMR spectra are very large (Fig. 2). They could correspond to **2a** and **2c** or to **2b** and **2b′** in rapid equilibrium (Scheme 9). However, only an equilibrium between **2b** and **2b′** is consistent with a dynamic process due to SSPT.

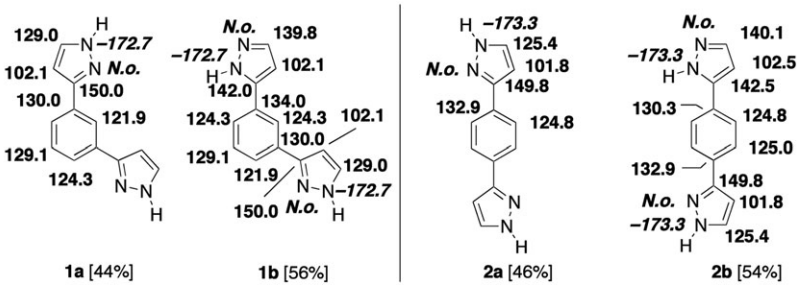

Scheme 7 ^{13}C and ^{15}N NMR signals (the latter in italics). N.o. not observed.

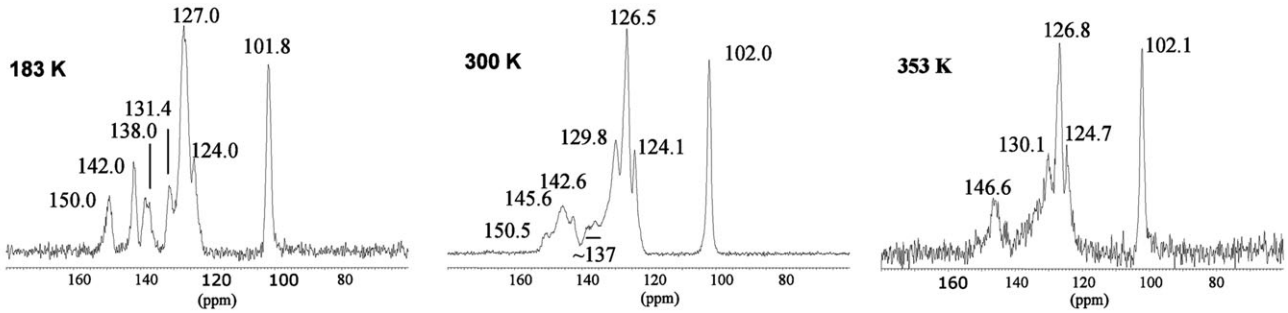

Fig. 2 ^{13}C CP-MAS spectra of **2** at 183, 300 (standard conditions, 27 °C) and 353 K.

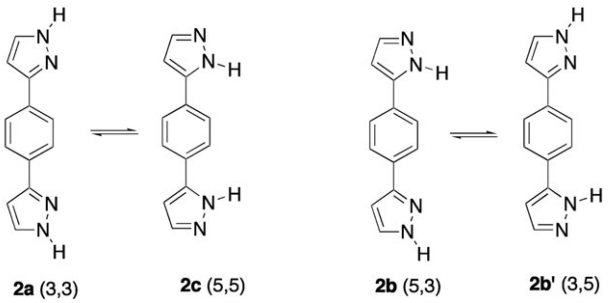

Scheme 9 The possible equilibria present in **2**.

From the separation of signals of pyrazole carbons CH and CAr (Scheme 10) at positions 3(5), 1460 and 725 Hz (14.5 and 7.2 ppm), and the coalescence temperatures (about 290 and 275 K), there is an interconversion barrier of about 50 kJ mol^{-1}, which is slightly higher than the highest barriers found in simple pyrazoles (Schemes 1 and 2), between 32.5 and 48.1 kJ mol^{-1}.[15] At 300 K there seem to be two kinds of cyclamers, one that coalesces and another that is only considerably broadened.

(b) ^{15}N NMR. In ^{15}N CP-MAS NMR, tautomer **1a** presents two broad signals at −102.8 (N2) and −163.6 ppm (N1)

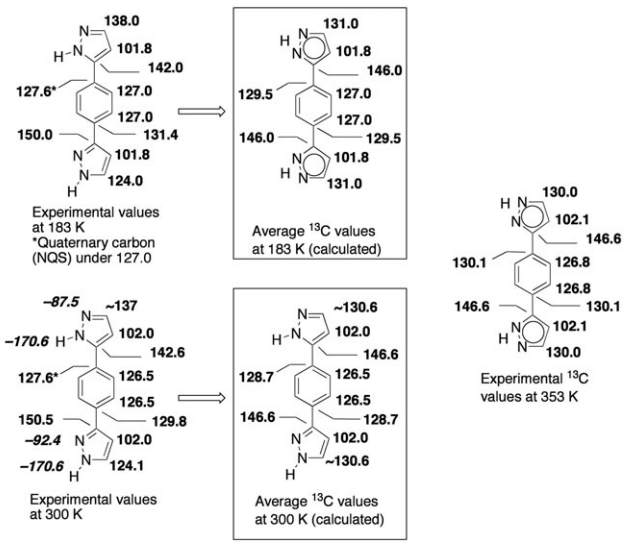

Scheme 10 ^{13}C and ^{15}N CP-MAS chemical shifts of tautomer **2b**. The experimental signal at 145.6 ppm (300 K) corresponds to the average signal calculated to be at 146.6 ppm.

(assigned by analogy with other pyrazoles).[16] They are shifted with respect to other values of ^{15}N chemical shifts of *NH*-pyrazoles in the solid state,[16] this being probably due to the inclusion of solvent molecules (the data correspond to the ethyl acetylacetate complex).

For compound **2b** in ^{15}N CP-MAS, two large but split signals are observed at −87.5 and −92.4 ppm (N2) and another signal at −170.6 ppm (N1). They correspond to both tautomers in a medium rate exchange, the 3-aryl part at −92.4 and −170.6 and the 5-aryl part at −87.5 and −170.6 ppm. The exchange rate seems slower in the NMR time-scale because the signals are closer (in Hz) in ^{13}C than in ^{15}N.

Having assigned all the signals to tautomers **1a** and **2b** it is possible now to compare them to the calculated δ values (obtained from the GIAO σ values in the gas-phase) The following three equations are obtained (three ^{15}N chemical shift values in solution are not sufficient for a regression analysis):

$$\delta(^{13}\text{C exp. solution}) = (6.2 \pm 2.7) + (0.95 \pm 0.02)\,\delta(^{13}\text{C calc.});\ n = 33,\ r^2 = 0.985 \quad (1)$$

$$\delta(^{13}\text{C exp. solid state}) = (7.5 \pm 4.7) + (0.94 \pm 0.04)\,\delta(^{13}\text{C calc.});\ n = 19,\ r^2 = 0.975 \quad (2)$$

$$\delta(^{15}\text{N exp. solid state}) = -(39.3 \pm 5.4) + (0.67 \pm 0.04)\,\delta(^{15}\text{N calc.});\ n = 6,\ r^2 = 0.988 \quad (3)$$

The 0.67 slope found in the third case means that the N–H···N hydrogen bonds present in the solid state profoundly perturb both N1 and N2 chemical shifts.

To compare the absolute shieldings obtained for the gas-phase with those obtained for DMSO with the PCM model, we calculate regressions (4)–(9).

$$\delta(^{13}\text{C exp. solution}) = (172.8 \pm 1.0) + (0.91 \pm 0.02)\,\sigma(^{13}\text{C calc. gas});\ n = 33,\ r^2 = 0.985 \quad (4)$$

$$\delta(^{13}\text{C exp. solid state}) = (173.2 \pm 1.9) + (0.91 \pm 0.04)\,\sigma(^{13}\text{C calc. gas});\ n = 19,\ r^2 = 0.975 \quad (5)$$

$$\delta(^{15}\text{N exp. solid state}) = -(141.4 \pm 2.1) + (0.64 \pm 0.04)\,\sigma(^{15}\text{N calc. gas});\ n = 6,\ r^2 = 0.988 \quad (6)$$

$$\delta(^{13}\text{C exp. solution}) = (172.0 \pm 1.5) + (0.91 \pm 0.03)\,\sigma(^{13}\text{C calc. DMSO–PCM});\ n = 33,\ r^2 = 0.971 \quad (7)$$

$$\delta(^{13}\text{C exp. solid state}) = (171.8 \pm 2.2) + (0.90 \pm 0.04)\,\sigma(^{13}\text{C calc. DMSO–PCM});\ n = 19,\ r^2 = 0.961 \quad (8)$$

$$\delta(^{15}\text{N exp. solid state}) = -(141.0 \pm 2.3) + (0.77 \pm 0.05)\,\sigma(^{15}\text{N calc. DMSO–PCM});\ n = 6,\ r^2 = 0.986 \qquad (9)$$

For this particular series of compounds, the calculation of absolute shieldings using the PCM model for DMSO as solvent does not improve the correlations.

Solid-state structures of 1 and 2

3,3′-(1,3-Phenylene)bis-1*H*-pyrazole (**1**) crystallizes from ethyl acetate–diethyl ether in the monoclinic space group $P2_1/n$. There are three crystallographically independent molecules and one additional disordered molecule of diethylether in the asymmetric unit. The molecular structure of the asymmetric is shown in Fig. 3. The pyrazoles are connected by hydrogen bonds in trimers, whereby two of the 3,3′-(1,3-phenylene)bis-1*H*-pyrazoles form parallel strands and the third molecule bridges these strands, which finally results in the formation of an eaves gutter-like structure (Fig. 4). Details of the hydrogen bonds are summarized in Table 2, crystal and refinement data are summarized in Table 4. The disordered molecule of diethyl ether occupies the cavity between the strand-bridging 3,3′-(1,3-phenylene)bis-1*H*-pyrazoles.

3,3′-(1,4-Phenylene)bis-1*H*-pyrazole (**2**) crystallizes from ethyl acetate in the monoclinic space group $C2/c$ with eight crystallographically equivalent molecules in the unit cell. The molecular structure of **2** is shown in Fig. 5. Both pyrazole substituents are involved in the formation of hydrogen bound tetramers leading to a remarkable structure with double stranded zigzag chains (Fig. 6). Details of the hydrogen bonds are summarized in Table 3, crystal and refinement data are summarized in Table 4.

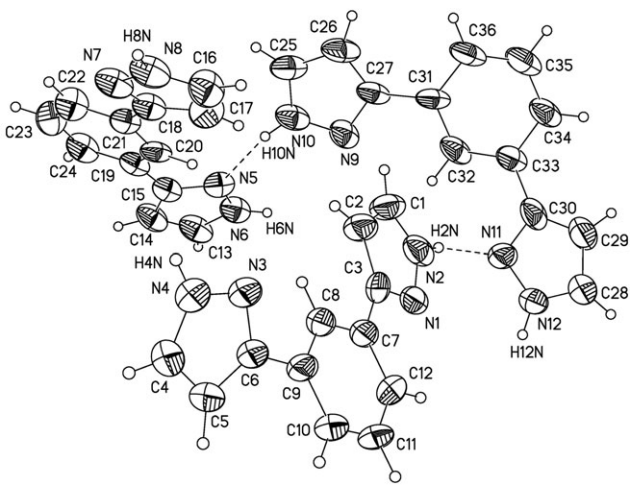

Fig. 3 Details of the solid-state structure of **1**. Top: view upon the bridged double strands including the disordered diethylether molecules; bottom: view perpendicular to the *ac*-plane. Characteristic hydrogen bond lengths (Å) and angles (°): N2–H2N 1.04(6), H2N···N11 1.83(6), N2···N11 171(5), N4–H4N 1.16(6), H4N···N1 1.77(6), N4···N1 2.917(6), N6–H6N 0.93(5), H6N···N7 1.98(5), N6···H6N 2.906(6), N8–H8N 1.24(6), H8N···N9 1.64(6), N8···N9 2.877(6), N10–H10N 1.36(7), H10N···N5 1.51(7), N10···N5 2.855(5), N12–H12N 1.03(6), H12N···N3 1.82(6), N12···N3 2.847(6); N2–H2N···N11 171(5), N4–H4N···N1 171(5), N6–H6N···N7 176(4), N8–H8N···N9 170(4), N10–H10N···N5 172(5), N12–H12N···N3 173(4).

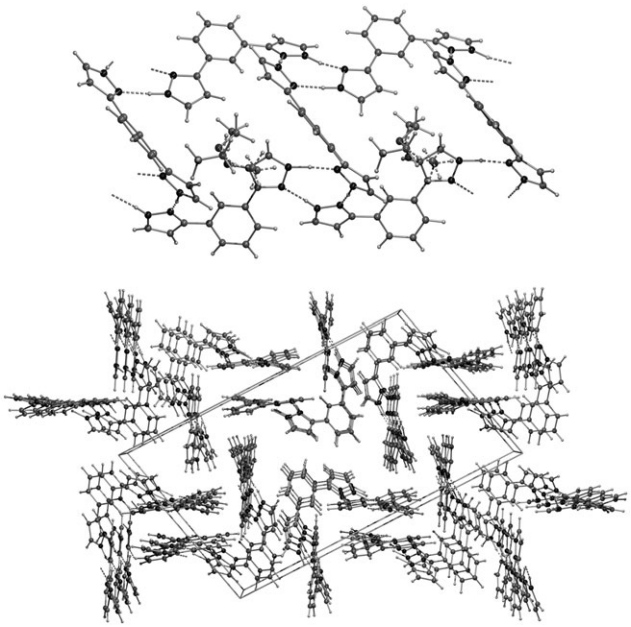

Fig. 4 Details of an isolated zigzag chain formed in the solid state structure of **2**. Top: side view; bottom: view perpendicular onto a pyrazole tetramer. Characteristic hydrogen bond lengths (Å) and angles (°): N2–H2N 0.76(3), H2N···N2 2.15(3), N2···N2 2.880(2), N3–H3N 0.83(3), H3N···N3 2.06(3), N3···N3 2.861(2), N4–H4N 0.82(4), H4N···N1 2.14(4), N4···N1 2.937(2); N2–H2N···N2 162(4), N3–H3N···N3 162(2), N4–H4N···N1 163(4).

Table 2 Geometrical details (bond lengths (Å), bond angles (°)) of intermolecular hydrogen bonds within the crystal structure of **1**

D–H···A	D–H	H···A	D···A	D–H···A
N2–H2N···N11	0.88	2.04	2.881(5)	159
N4–H4N···N1	0.88	2.07	2.937(5)	167
N6–H6N···N7	0.88	2.04	2.914(5)	171
N8–H8N···N9	0.88	2.08	2.892(5)	152
N10–H10N···N5	0.88	2.02	2.872(5)	163
N12–H12N···N3	0.88	2.00	2.853(5)	162

For each pyrazole tetramer, there are two possible orientations of the hydrogen bonds. This leads to a statistical disorder of these hydrogen bond arrangements in the crystal and is expressed in Fig. 4 by two positions for each N–H···N unit. Therefore the drawing must not be interpreted as a fully free disordering of the protons in the tetramers. The formation of the double stranded chains allows the π–π stacking of pairs of phenylene units, which further stabilizes the solid state structure resulting in a remarkably high melting point of 297 °C.

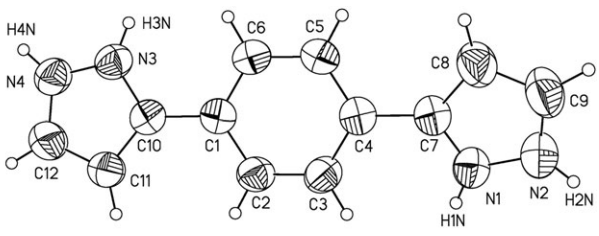

Fig. 5 ORTEP (50% probability level) of the molecular structure of **2**.

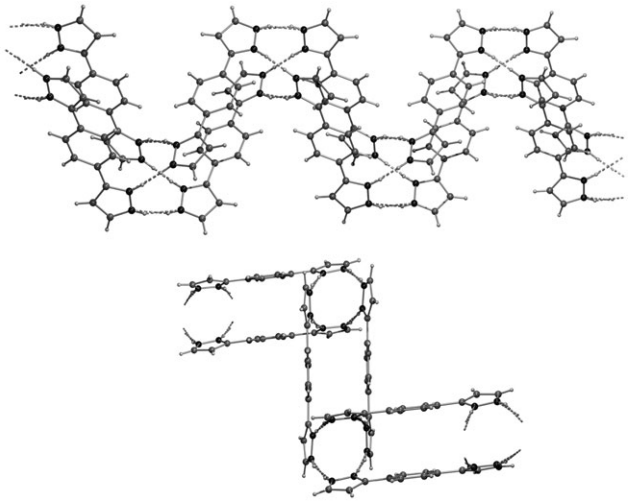

Fig. 6 Details of an isolated zigzag chain formed in the solid-state structure of **2**. Top: side view; bottom: view perpendicular onto a pyrazole tetramer.

Table 3 Geometrical details (bond lengths (Å), bond angles (°)) of intermolecular hydrogen bonds within the crystal structure of **2**

D–H···A	D–H	H···A	D···A	D–H···A
N1–H1N···N4	0.86	2.10	2.936(2)	164
N2–H2N···N2	0.86	2.12	2.870(2)	146
N3–H3N···N3	0.86	2.05	2.862(2)	158
N4–H4N···N1	0.86	2.14	2.936(2)	153

Table 4 Crystal data and structure refinement of **1** and **2**

	1	**2**
Chemical formula	$C_{40}H_{40}N_{12}O$	$C_{12}H_{10}N_4$
Formula weight	704.84	210.24
Space group	$P2_1/n$	$C2/c$
a/Å	15.3449(19)	10.4886(11)
b/Å	9.6588(12)	12.8375(13)
c/Å	26.538(3)	15.7298(17)
γ/°	106.190(2)	101.024(2)
V/Å^3	3777.3(8)	2078.9(4)
Z	4	8
θ Range for data collection	1.60–26.02	2.78–25.74
Index ranges, hkl	−18 to 16, −8 to 11, −5 to 32	−12 to 12, −15 to 15, −19 to 19
Total/independent reflections	13355/6804 (R_{int} = 0.1093)	9102/2038 (R_{int} = 0.0291)
Data/restraints/parameters	6804/218/527	2038/0/163
Goodness-of-fit on F^2	0.801	1.056
Final R indices [$I > 2\sigma(I)$]	R_1 = 0.0666, wR_2 = 0.1120	R_1 = 0.0423, wR_2 = 0.1141

Conclusions

Concerning tautomerism in solution, the compounds reported in this study behave similarly tautomers **a** and **b** being present in an almost 1:1 ratio. In the solid state there are important differences. The *meta* derivative **1** exists as 3,3-substituted tautomer **1a** in a static situation as shown both by CP-MAS NMR and X-ray crystallography. Although there are only three independent molecules in the unit cell, the splitting observed in ^{13}C NMR is higher than 3, probably 6, indicating small conformational differences for each molecule; however, other factors such as quadrupolar nuclei, could influence the splitting. On the other hand, the *para* derivative **2** exists as the 3,5-substituted tautomer **2b** and presents SSPT with a barrier about 50 kJ mol^{-1}. This implies that this compound forms cyclamers, however CP-MAS NMR does not allow to determine its nature: a dimer $(\mathbf{2b})_2$, a trimer $(\mathbf{2b})_3$ or a tetramer $(\mathbf{2b})_4$. X-Ray crystallography shows both disorder and tetramers (8 equivalent molecules), proving once again the extraordinary complementarity of these two techniques.

It is worth mentioning that in the related case of the *para* derivative **4** (R = *t*-Bu), the X-ray structure has been determined and corresponds to a 3,3-tautomer without proton disorder (**4a**).[10] Up to now, it is still very difficult to design molecules showing SSPT, because similar compounds form very different hydrogen-bonded networks.

The use of the PCM model does not represent an improvement neither in the energies nor in the absolute shieldings.

Experimental

Compounds **1** and **2** were prepared according to ref. 9. ^{1}H NMR (DMSO-d_6 15.5 mg, 0.5 mL): **1a**, 6.76 (H4, d, J = 2.0 Hz), 7.43 (H5 and H5′, m), 7.72 (H4′ and H6′, m), 8.22 (H2′, s), 12.90 (NH); **1b**, 6.76 (H4 and H4″, m), 7.43 (H3″, H5 and H5′, m), 7.5 (H4′, very broad), 7.78 (H2′, s), 8.1 (H6′, very broad), 12.90 and 13.34 (NH); **2a** 6.72 (H4, d, J = 2.0 Hz), 7.6 (H5, very broad), 7.83 (H2′, broad), 12.90 (NH); **2b** 6.72 (H4, d, J = 2.0 Hz), 6.68 (H4″, d, J = 1,7 Hz), 7.46 (H3″ and H3′, broad), 7.6 (H5, very broad), 7.83 (H2′, broad), 12.90 and 13.30 (NH).

X-Ray crystallography

Two structures (compounds **1** and **2**) have been recorded at low temperature (**1**: 173 K, **2**: 183 K) on a Bruker Smart CCD 1 k diffractometer equipped with an Oxford Cryosystems Cryostream Cooler Device using a graphite-monochromated Mo-Kα radiation (λ = 0.71073 Å). Data collection, data reduction and refinement of the structures proceeded smoothly. Both structures were solved by direct methods with SHELXS-97[17] and refined by full-matrix least-squares procedures on F^2, using the program SHELXL-97.[18] All non-hydrogen atoms were refined anisotropically. All hydrogen atom positions were refined using a riding model. For compound **1** the atoms of the diethyl ether molecule were refined disordered over two positions with occupation factors of 0.55 (C37–C40, O1) and 0.45 (C37′–C40′, O1′). For compound **2** the *N*-bonded hydrogen atoms were refined disordered with occupation factors of each 0.50. Table 4 contains a summary of crystal and refinement data and details can be found as ESI.† Drawing of molecules (Fig. 3 and 4) was performed with the program PLUTON.[19]

CCDC reference numbers 679321 (**1**) and 679322 (**2**).

For crystallographic data in CIF or other electronic format see DOI: 10.1039/b803855d

NMR Experiments

Solution NMR spectra. Solution NMR spectra were recorded on a Bruker DRX 400 (9.4 Tesla, 400.13 MHz for ^{1}H, 100.62 MHz for ^{13}C and 40.56 MHz for ^{15}N) spectrometer with a 5 mm inverse detection H-X probe equipped with a z-gradient coil, at 300 K. Chemical shifts (δ in ppm) are given from internal solvent, DMSO-d_6 2.49 for ^{1}H and 39.5 for ^{13}C, and for ^{15}N NMR nitromethane (0.00) were used as external standards. Typical parameters for ^{1}H NMR spectra were spectral width 5787 Hz, pulse width 7.5 μs at an attenuation level of 0 dB and resolution 0.34 Hz per point. For ^{13}C NMR spectra, spectral width 21 kHz, pulse width 10.6 μs at an attenuation level of −6 dB, relaxation delay 2 s, resolution 0.63 Hz per point; WALTZ-16 was used for broadband proton decoupling; the FIDS were multiplied by an exponential weighting (lb = 1 Hz) before Fourier transformation. 2D inverse proton detected heteronuclear shift correlation spectra, gs-HMQC (^{1}H–^{13}C) and gs-HMBC (^{1}H–^{13}C) were acquired and processed using standard Bruker NMR software. Selected parameters for (^{1}H–^{13}C) gs-HMQC and gs-HMBC spectra were: spectral width 5787 Hz for ^{1}H and 20.5 kHz for ^{13}C, 1024 × 256 data set, number of scans 2 (gs-HMQC) or 4 (gs-HMBC), relaxation delay 1 s, and delay for the evolution of ^{13}C–^{1}H coupling constants of 3 ms (gs-HMQC) and 60 ms (gs-HMBC). The FIDs were processed using zero filling in the *F*1 domain and a sine-bell window function in both dimensions was applied prior to Fourier transformation. In the gs-HMQC experiments GARP modulation of ^{13}C was used for decoupling. ^{15}N NMR was acquired using 2D inverse proton detected heteronuclear shift correlation spectra, selected parameters for gs-HMQC (^{1}H–^{15}N) spectra were: spectral width 5787 Hz for ^{1}H and 12.5 kHz for ^{15}N, 1024 × 256 data set, number of scans 4, relaxation delay 1 s, 7 ms delay for the evolution of the ^{15}N–^{1}H coupling. The FIDs were processed using zero filling in the *F*1 domain and a sine-bell window function in both dimensions was applied prior to Fourier transformation.

Solid-state NMR spectra. ^{13}C (100.73 MHz) and ^{15}N (40.60 MHz) CP-MAS NMR spectra were obtained on a Bruker WB 400 spectrometer at 300 K using a 4 mm DVT probehead. Samples were carefully packed in a 4-mm diameter cylindrical zirconia rotors with Kel-F caps. Operating conditions involved 3.2 μs 90 ^{1}H pulses and decoupling field strength of 78.1 kHz by TPPM sequence. The NQS (Non-Quaternary Suppression) technique to observe only the quaternary C-atoms was employed. ^{13}C spectra were originally referenced to a glycine sample and then the chemical shifts were recalculated to the Me_4Si (for the carbonyl atom δ(glycine) = 176.1 ppm) and ^{15}N spectra to $^{15}NH_4Cl$ and then converted to nitromethane scale using the relationship: δ(^{15}N nitromethane) = δ(^{15}N ammonium chloride) – 338.1 ppm. Typical acquisition parameters for ^{13}C CP-MAS were: spectral width, 40 kHz; recycle delay, 15–75 s; acquisition time, 30 ms; contact time, 2 ms; and spin rate, 12 kHz, and for ^{15}N CP-MAS: spectral width, 40 kHz; recycle delay, 15–75 s; acquisition time, 35 ms; contact time, 7–8 ms; and spin rate, 6 kHz.

A Bruker BVT3000 temperature unit was used to control the temperature of the cooling gas stream an a exchanger to achieve low temperatures. To avoid problems caused by air moisture, pure nitrogen was used as bearing, driving and cooling gas; zirconia caps were used.

Computational details

The geometry of the complexes has been optimized at the B3LYP/6-31G(d)[20,21] computational level using the ultrafine keyword and the Gaussian 03 package.[22] Frequency calculation at the same computational level has been carried out to confirm that the structures obtained correspond to energetic minima. A further geometry optimization has been performed at the B3LYP/6-311 + + G(d,p).[23] The absolute chemical shielding has been obtained at the B3LYP/6-311 + + G(d,p) level using the GIAO method.[24] The energies included the zero point energy (ZPE) correction. In all cases the calculated values are consistent with the assignment based on 2D experiments.

Acknowledgements

Thanks are given to MCyT of Spain for financial support, project number CTQ2007-62113 as well as to Comunidad Autónoma de Madrid (Project MADRISOLAR, ref. S-0505/PPQ/0225).

References

1 (*a*) J. Elguero, *Comprehensive Heterocyclic Chemistry II*, ed. A. R. Katritzky, C. W. Rees and E. F. V. Scriven, Pergamon-Elsevier, Oxford, vol. 3, 1996, pp. 1–75; (*b*) V. I. Minkin, A. D. Garnovskii, J. Elguero, A. R. Katritzky and O. V. Denisko, *Adv. Heterocycl. Chem.*, 2000, **76**, 157–323.
2 (*a*) M. A. P. Martins, N. Zanatta, H. G. Bonacorso, F. A. Rosa, R. M. Claramunt, M. A. García, M. D. Santa María and J. Elguero, *Arkivoc*, 2006, **iv**, 29–37; (*b*) I. Alkorta, J. Elguero and J. F. Liebman, *Struct. Chem.*, 2006, **17**, 439–444; (*c*) R. M. Claramunt, P. Cornago, V. Torres, E. Pinilla, M. R. Torres, A. Samat, V. Lokshin, M. Valés and J. Elguero, *J. Org. Chem.*, 2006, **71**, 6881–6891; (*d*) C. Foces-Foces, M. L. Rodríguez and J. Elguero, *Acta Crystallogr., Sect. E: Struct. Rep. Online* , 2006, **62**, o3351–o3353; (*e*) A. Levai, A. M. S. Silva, J. A. S. Cavaleiro, I. Alkorta, J. Elguero and J. Jeko, *Eur. J. Org. Chem.*, 2006, 2825–2832; (*f*) S. Trofimenko, G. P. A. Yap, F. A. Jové, R. M. Claramunt, M. A. García, M. D. Santa María, I. Alkorta and J. Elguero, *Tetrahedron*, 2007, **63**, 8104–8111; (*g*) P. Cornago, R. M. Claramunt, L. Bouissane and J. Elguero, *Tetrahedron*, 2008, **64**, 3667–3673.
3 (*a*) V. N. Kourafalos, P. Marakos, E. Mikros, N. Pouli, J. Marek and R. Marek, *Tetrahedron*, 2006, **62**, 11987–11993; (*b*) A. A. Gevorkyan, A. S. Arakelyan, G. V. Asratyan, A. G. Petrosyan, K. A. Petrosyan and G. A. Panosyan, *Hayastani Kim Handes*, 2006, **59**, 83–92; (*c*) Y. C. Shi, B. B. Zhu and C. X. Sui, *Acta Crystallogr., Sect. E: Struct. Rep. Online* , 2006, **62**, m2389–m2391; (*d*) F. Chimenti, R. Fioravanti, A. Bolasco, F. Manna, P. Chimenti, D. Secci, O. Befani, P. Turini, F. Ortuso and S. Alcaro, *J. Med. Chem.*, 2007, **50**, 425–428; (*e*) A. Kusakiewicz-Dawid, E. Masiukiewicz. B. Rzeszotarska, I. Dybala, A. E. Kozio and M. A. Broda, *Chem. Pharm. Bull.*, 2007, **55**, 747–752.
4 I. Alkorta and J. Elguero, *Top. Heterocycl. Chem.*, 2009, DOI: 10.1007/7081_2008_1.
5 R. M. Claramunt, C. López, M. D. Santa María, D. Sanz and J. Elguero, *Prog. Nucl. Magn. Reson. Spectrosc.*, 2006, **49**, 169–206.

6 (*a*) J. Elguero, N. Jagerovic, C. Foces-Foces, F. H. Cano, M. V. Roux, F. Aguilar-Parrilla and H.-H. Limbach, *J. Heterocycl. Chem.*, 1995, **32**, 451–456; (*b*) R. M. Claramunt, P. Cornago, M. D. Santa María, V. Torres, E. Pinilla, M. R. Torres and J. Elguero, *Supramol. Chem.*, 2006, **18**, 349–356.
7 Y. Lin and S. A. Lang, *J. Heterocycl. Chem.*, 1977, **14**, 345–347.
8 D. B. Grotjahn and D. Combs, *PCT Int. Appl.*, WO 20000056717 A1 28 Sep. 2000, *Chem. Abstr.*, 2000, **133**, 246521.
9 A.-K. Pleier, H. Glas, M. Grosche, P. Sirsch and W. R. Thiel, *Synthesis*, 2001, 55–62.
10 M. J. Hayter, D. J. Bray, J. K. Clegg and L. F. Lindoy, *Synth. Commun.*, 2006, **36**, 707–714.
11 S. Gemming, M. Schreiber, W. Thiel, T. Heine, G. Seifert, H. A. de Abreu and H. A. Duarte, *J. Lumin.*, 2004, **108**, 143–147.
12 M. A. García, C. López, R. M. Claramunt, A. Kenz, M. Pierrot and J. Elguero, *Helv. Chim. Acta*, 2002, **85**, 2763–2776.
13 F. F. Blanco, I. Alkorta and J. Elguero, *Magn. Reson. Chem.*, 2007, **45**, 797–800.
14 F. Reviriego, I. Alkorta and J. Elguero, *J. Mol. Struct.*, 2008, DOI: 10.1016/j.molstruc.2008.04.002.
15 O. Klein, F. Aguilar-Parilla, J. M. López, N. Jagerovic, J. Elguero and H.-H. Limbach, *J. Am. Chem. Soc.*, 2004, **126**, 11718–11732.
16 R. M. Claramunt, D. Sanz, C. López, J. A. Jiménez, M. L. Jimeno, J. Elguero and A. Fruchier, *Magn. Reson. Chem.*, 1997, **35**, 35–75.
17 G. M. Sheldrick, *Acta Crystallogr., Sect. A: Found. Crystallogr.*, 1990, **46**, 467.
18 G. M. Sheldrick, SHELXL-97: A program for crystal structure refinement, University of Göttingen, Germany, 1997, Release 97-2.
19 PLUTON plot with POVRAY version 3.6: A. L. Spek, *PLUTON. A program for plotting molecular and crystal structures*, University of Utrecht, The Netherlands, 1995.
20 (*a*) A. D. Becke, *Phys. Rev. A: At., Mol., Opt. Phys.*, 1988, **38**, 3098–3100; (*b*) A. D. Becke, *J. Chem. Phys.*, 1993, **98**, 5648–5652; (*c*) C. Lee, W. Yang and R. G. Parr, *Phys. Rev. B: Condens. Matter Mater. Phys.*, 1988, **37**, 785–789.
21 P. A. Hariharan and J. A. Pople, *Theor. Chim. Acta*, 1973, **28**, 213–222.
22 M. J. Frisch, G. W. Trucks, H. B. Schlegel, G. E. Scuseria, M. A. Robb, J. R. Cheeseman, J. A. Montgomery, Jr, T. Vreven, K. N. Kudin, J. C. Burant, J. M. Millam, S. S. Iyengar, J. Tomasi, V. Barone, B. Mennucci, M. Cossi, G. Scalmani, N. Rega, G. A. Petersson, H. Nakatsuji, M. Hada, M. Ehara, K. Toyota, R. Fukuda, J. Hasegawa, M. Ishida, T. Nakajima, Y. Honda, O. Kitao, H. Nakai, M. Klene, X. Li, J. E. Knox, H. P. Hratchian, J. B. Cross, C. Adamo, J. Jaramillo, R. Gomperts, R. E. Stratmann, O. Yazyev, A. J. Austin, R. Cammi, C. Pomelli, J. W. Ochterski, P. Y. Ayala, K. Morokuma, G. A. Voth, P. Salvador, J. J. Dannenberg, V. G. Zakrzewski, S. Dapprich, A. D. Daniels, M. C. Strain, O. Farkas, D. K. Malick, A. D. Rabuck, K. Raghavachari, J. B. Foresman, J. V. Ortiz, Q. Cui, A. G. Baboul, S. Clifford, J. Cioslowski, B. B. Stefanov, G. Liu, A. Liashenko, P. Piskorz, I. Komaromi, R. L. Martin, D. J. Fox, T. Keith, M. A. Al-Laham, C. Y. Peng, A. Nanayakkara, M. Challacombe, P. M. W. Gill, B. Johnson, W. Chen, M. W. Wong, C. Gonzalez and J. A. Pople, *GAUSSIAN 03*, Gaussian, Inc., Pittsburgh, PA, 2003.
23 (*a*) R. Ditchfield, W. J. Hehre and J. A. Pople, *J. Chem. Phys.*, 1971, **54**, 724–728; (*b*) M. J. Frisch, J. A. Pople, R. Krishnam and J. S. Binkley, *J. Chem. Phys.*, 1984, **80**, 3265–3269.
24 R. Ditchfield, *Mol. Phys.*, 1974, **27**, 789–807; F. London, *J. Phys. Radium*, 1937, **8**, 397–409.

